



# SCATTERING OF A SPHERICAL WAVE BY A THIN HARD STRIP

D. OUIS

*Department of Engineering Acoustics, Lund Institute of Technology,  
P.O. Box 118, S-221 00, Lund, Sweden*

*(Received 20 March 1998, and in final form 4 August 1998)*

This paper is concerned with a theoretical solution to the problem of scattering of a spherical wave by a strip. The strip is infinitely thin, infinite in length and of width  $2a$ . The problem is first brought into the wave space through a spatial Fourier transform of the wave equation and of the boundary conditions on the strip. The Fourier transform is taken with respect to the co-ordinate axis parallel to the edges of the strip. Using the boundary conditions on the strip leads to an integral equation of the first kind, the unknown of which is the discontinuous potential jump across the strip. This latter is expanded into some suitable functions and the coefficients of the series expansion are thereafter determined from an infinite system of equations. The system's matrix is found to be mainly diagonal and tests on the stability of the numerical calculations suggest the significant number of equations in the system be limited to approximately  $ka + 5$ , with  $k$  being the wavenumber. Finally, after solving the system of equations and going back to the scattered field, the expression of this latter is made from an infinite series over some infinite double integrals whose approximate evaluation is made with the help of the two-dimensional stationary phase method. This treatment corresponds to the far field case. A further consideration of the right side of the system of equations leads to an improved value of the scattered field. Comparisons are made to an approximated prediction of the scattered field by using the Biot and Tolstoy exact theory of diffraction of a spherical wave by a hard wedge. The implementation of this approach to the strip requires the further consideration of the multiple diffraction between its edges for improving the calculated value of the scattered field. Some numerical examples are treated with discussions on their results.

© 1999 Academic Press

## 1. INTRODUCTION

The study of the scattering of waves by a strip has attracted the interest of theoreticians and experimenters for almost two centuries. Indeed, in problems of wave interaction with thin scatterers, the case of the strip is given special attention because it is considered as the simplest one after that of the half plane. This is due not only to the relatively simple shape of the strip but also because in studying for instance the problems of noise shielding by simple barriers, these latter are often, if not always, modelled as hard thin strips standing on the ground.

Moreover, the important principle of Babinet stipulates that the complementary problems of scattering by a disk and of that of a similar aperture in an infinite plane have equivalent solutions. In this latter case, the scattering problem of a slit in a screen can be formulated as that of two half planes in mutual interaction and for such approaches the strip is the simplest case to consider [1]. Unfortunately, and although extensive studies stretching in time over many decades have been made, none of the attempts to find exact solutions to the problem of the strip has been successful up to date in finding elegant closed form solutions like those elaborated for the half plane [2]. It may be of interest to note also that of the many reported results of studies in this spirit, one finds that most of them treat the case of plane or cylindrical wave incidence, thus making the problem easily amenable to a two dimensional analysis. However, in practical problems of sound scattering by thin hard objects and due to the relatively long wavelengths of sound, low frequencies are a major source of trouble and considering the more general case of the spherical source is therefore of prime importance.

Potential theory has been used earlier for solving either interior problems or problems of wave interaction with plane obstacles delimited by sharp edges [3, 4]. In this latter case, the field scattered by the obstacle may be represented as the potential of a single or a double layer on the scattering object, the density of which is to be determined through applying the pertaining boundary conditions on the scatterer. This approach is more reliable for this kind of problem, as its formulation is exact. However, for the case of a hard obstacle, which is of most interest in acoustics, the integral equation so obtained for the layer density, a Fredholm equation of the first kind, may be correctly formulated only through resorting to the theory of distributions. The solution of the integral equations so obtained requires also the careful use of some special techniques [4–6]. It could be of some interest to note that the problem of noise shadowing by a thin screen on a hard plane has also been formulated by a potential theory approach. The solution to this problem has given an excellent agreement between theoretically predicted and experimentally measured values of the scattered field [7].

In this paper, the problem of scattering of a spherical wave by a thin hard strip is approached through the solution of an integral equation in the potential jump across the thin strip. A similar approach has been successfully used by Boström to solve the problem of plane wave scattering by a thin hard rectangle [8], and by Boström and Peterson for the case of a thin hard circular disk [9] at the separation between two fluids. It is found that with relatively light computing efforts, the solution presented here for the problem of the strip in the field of a spherical wave is very satisfactory for most engineering purposes. In section 2 of this paper the problem is formulated and in section 3 the final formulation is given for the integral equation for the potential jump which is the unknown quantity. Section 4 presents the solution of the integral equation with some details on the diverse approximations and the improvements caused to the value of the scattered field. Subsequently, in section 5 an approximate solution is formulated for the field scattering by the strip in terms of an exact solution for the half plane by using the generalized Biot–Tolstoy theory of spherical wave diffraction by a hard wedge. The single diffraction approach applied to the edges of the strip is then

supplemented by a multi-diffraction algorithm to take into account the mutual interaction of the strip edges. Finally, section 6 is devoted to some numerical examples with discussions on their results.

### 2. FORMULATION OF THE PROBLEM

Consider the thin hard strip in the  $xOz$  plane, with its edges parallel to the  $z$ -axis and at  $x = \pm a$ ; see Figure 1. The point sound source with co-ordinates  $S(x_s, y_s, 0)$  is assumed to have the time harmonic dependence  $e^{-i\omega t}$  and the observation point is  $R(x, y, z)$ . The sound speed in the fluid is  $c$  and  $k$  is the wavenumber.

The problem is then to solve the Helmholtz wave equation:

$$\nabla^2 u + k^2 u = 0 \tag{1}$$

subject to the Neumann boundary conditions on the hard strip. Hence, if  $u$  denotes the potential scattered by the strip, i.e., the potential which is the contribution to the total field due to the presence of the strip, then

$$\frac{\partial u}{\partial y} = -\frac{\partial u^i}{\partial y} \quad \text{for } |x| \leq a \quad \text{and } y = 0, \tag{2}$$

where  $u^i$  is the spherical incident wave:

$$u^i = e^{ikR}/R, \quad R = [(x - x_s)^2 + (y - y_s)^2 + z^2]^{1/2}. \tag{3}$$

The scattering problem as formulated here must also be complemented by some radiation conditions at infinity to ensure the uniqueness of the solution.

### 3. INTEGRAL EQUATION FOR THE SCATTERING PROBLEM

To solve the scattering problem, equations (1) and (2) are brought into the Fourier domain and an appropriate choice is made for the expression of the Fourier transformed scattered field  $\bar{u}$ . First, it is necessary to give a definition of the Fourier transform and its inverse:

$$\bar{u} = \frac{1}{\sqrt{2\pi}} \int_{-\infty}^{+\infty} u e^{-ipz} dz \Leftrightarrow u = \frac{1}{\sqrt{2\pi}} \int_{-\infty}^{\infty} \bar{u} e^{ipz} dp. \tag{4}$$

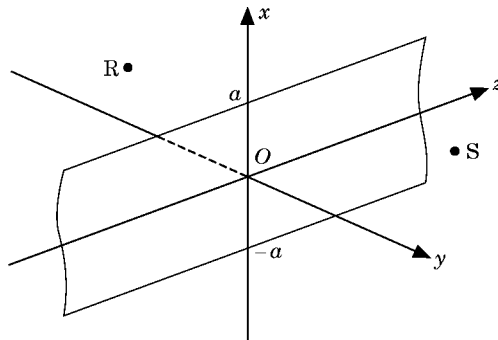


Figure 1. Geometry for the problem of scattering of a spherical wave by a thin strip.

Applying the direct transform to equations (1) and (2) gives

$$\partial^2 \bar{u} / \partial x^2 + \partial^2 \bar{u} / \partial y^2 + (k^2 - p^2) \bar{u} = 0, \quad (5)$$

$$\frac{\partial \bar{u}}{\partial y} = -\frac{\partial}{\partial y} \frac{1}{\sqrt{2\pi}} \int_{-\infty}^{\infty} \frac{e^{ikR}}{R} e^{-ipz} dz, \quad |x| \leq a, y = 0. \quad (6)$$

In this last equation, the integration is carried out by using

$$\int_{-\infty}^{\infty} \frac{e^{ikR}}{R} e^{-ipz} dz = i\pi H_0^{(1)}(\bar{R}\sqrt{k^2 - p^2}), \quad (7)$$

where  $H_0^{(1)}$  is the Hankel function of the first kind and of zero order and

$$\bar{R} = [(x - x_s)^2 + (y - y_s)^2]^{1/2}. \quad (8)$$

It is assumed that the solution of equation (5) can be put into the form

$$\bar{u} = \frac{\text{sgn}(y)}{\sqrt{2\pi}} \int_{-\infty}^{\infty} f(q, p) e^{i(qx + h|y|)} dq, \quad (9)$$

with

$$h = \sqrt{k^2 - q^2 - p^2}, \quad \text{Im}(h) \geq 0. \quad (10)$$

The form of the scattered field as given in equations (9) and (10) ensures that it satisfies both the wave equation and the radiation condition. Moreover, the continuity of its  $y$ -gradient is fulfilled everywhere in space.

For  $y = 0$ , the potential  $\bar{u}$  is continuous away from the strip and makes a so far unknown jump  $\Delta \bar{u}$  across it:

$$\bar{u}_{y=0+} - \bar{u}_{y=0-} = \sqrt{\frac{2}{\pi}} \int_{-\infty}^{\infty} f(q, p) e^{iqx} dq = \begin{cases} \Delta \bar{u}, & |x| \leq a \\ 0, & |x| > a \end{cases}. \quad (11)$$

Inverse Fourier transforming equation (11) gives then

$$f(q, p) = \frac{1}{2\sqrt{2\pi}} \int_{-a}^a \Delta \bar{u} e^{-iqx} dx. \quad (12)$$

The continuity of the  $y$ -derivative of the field across the strip can be formulated as

$$\left. \frac{\partial \bar{u}}{\partial y} \right|_{y=0} = \frac{1}{\sqrt{2\pi}} \int_{-\infty}^{\infty} f(q, p) ih e^{iqx} dq, \quad (13)$$

which, when used in equation (6) along with the property (7), leads to an integral equation for the unknown function  $f(q, p)$ :

$$\int_{-\infty}^{\infty} f(q, p) h e^{iqx} dq = -\pi \frac{\partial}{\partial y} H_0^{(1)}(\bar{R}\sqrt{k^2 - p^2})|_{y=0}, \quad |x| \leq a, \quad (14)$$

or if one is interested in solving for the Fourier transformed potential jump  $\Delta\bar{u}$ ,

$$\frac{1}{(2\pi)^{3/2}} \int_{-\infty}^{\infty} \int_{-a}^a \Delta\bar{u}(x', p) e^{-iqx'} dx' h(q, p) e^{iqx} dq = -\frac{\partial}{\partial y} H_0^{(1)}(\bar{R}\sqrt{k^2 - p^2})|_{y=0},$$

$$|x| \leq a. \quad (15)$$

#### 4. SOLUTION OF THE INTEGRAL EQUATION

To solve the integral equation (15),  $\Delta\bar{u}$  may be expanded in some suitable way. First, one can introduce the Chebychev ‘‘polynomials’’  $\varphi_n(x)$  which are defined by

$$\varphi_n(x) = \begin{cases} \cos(n \arcsin x) & n = 1, 3, 5, \dots \\ i \sin(n \arcsin x) & n = 2, 4, 6, \dots \end{cases} \quad (16)$$

and expand  $\Delta\bar{u}$  in them: i.e.,

$$\Delta\bar{u} = \sum_{n=1}^{\infty} \alpha_n(p) \varphi_n\left(\frac{x}{a}\right). \quad (17)$$

Actually, the functions  $\varphi_n$  are not polynomials but they are related to the true Chebychev polynomials  $T_n$  and  $U_n$ . The choice of the expansion in the  $\varphi_n$ s is made in order to describe correctly the square root behaviour of the surface field at the edges of the scattering plane strip: that is, with reference to Figure 1, the form  $[1 - (x/a)^2]^{1/2}$  for the surface potential is preserved as  $x \rightarrow a$  [10]. Hence, with this form of the potential jump, it is possible to perform analytically the inner integrals in equation (15) through using (see the Appendix)

$$\int_{-a}^a \varphi_n\left(\frac{x}{a}\right) e^{-iqx} dx = \frac{n\pi}{q} J_n(qa), \quad (18)$$

in which  $J_n$  denotes the Bessel function of the first kind and of order  $n$ . Equation (12) can then be written again as

$$f(q, p) = \frac{1}{2\sqrt{2\pi}} \int_{-a}^a \Delta\bar{u} e^{-iqx} dx = \frac{1}{2q} \sqrt{\frac{\pi}{2}} \sum_{n=1}^{\infty} n \alpha_n(p) J_n(qa), \quad (19)$$

and setting the expansion (17) for  $\Delta\bar{u}$  in equation (15), whereafter use is made of the property (18) leads to

$$\frac{\pi}{(2\pi)^{3/2}} \sum_{n=1}^{\infty} n\alpha_n(p) \int_{-\infty}^{\infty} \frac{h}{q} J_n(qa) e^{iqx} dq = -\frac{\partial}{\partial y} H_0^{(1)}(\bar{R}\sqrt{k^2-p^2})|_{y=0}, \quad |x| \leq a. \quad (20)$$

Next, a multiplication of both sides of equation (20) by  $\varphi_m(x/a)$  and an integration from  $-a$  to  $a$ , with use of (see the Appendix)

$$\int_{-a}^a \varphi_m\left(\frac{x}{a}\right) e^{iqx} dx = (-1)^{m-1} \frac{m\pi}{q} J_m(qa), \quad (21)$$

permits one to express equation (20) in a new form, namely

$$\begin{aligned} (-1)^m \frac{m}{2} \sqrt{\frac{\pi}{2}} \sum_{n=1}^{\infty} n\alpha_n(p) \int_{-\infty}^{\infty} \frac{h}{q^2} J_n(qa) J_m(qa) dq \\ = \int_{-a}^a \varphi_m\left(\frac{x}{a}\right) \frac{\partial}{\partial y} H_0^{(1)}(\bar{R}\sqrt{k^2-p^2})|_{y=0} dx, \quad |x| \leq a. \end{aligned} \quad (22)$$

Note that  $h$  is dependent on  $q$  through equation (10).

By varying  $m$  in equation (22), one gets an infinite system of linear equations to be solved,

$$\sum_{n=1}^{\infty} Q_{nm}\alpha_n = T_m \quad 1 \leq m \leq \infty, \quad (23)$$

where

$$Q_{nm} = (-1)^m \frac{nm}{2} \sqrt{\frac{\pi}{2}} \int_{-\infty}^{\infty} \frac{\sqrt{k^2-q^2-p^2}}{q^2} J_n(qa) J_m(qa) dq \quad (24)$$

and

$$T_m = \int_{-a}^a \varphi_m\left(\frac{x}{a}\right) \frac{\partial}{\partial y} H_0^{(1)}(\bar{R}\sqrt{k^2-p^2})|_{y=0} dx. \quad (25)$$

The scattering problem is then solved by first calculating the expansion coefficients  $\alpha_n$  from equation (23), then setting them into the expression for the potential jump in equation (17), which in turn gives form to the function  $f(q, p)$  in equation (12). Thereafter, the Fourier transformed scattered field  $\bar{u}$  is evaluated according to

equation (9), which lastly leads to the scattered field  $u$  through equation (4) or, all operations having been made,

$$u = \frac{\text{sgn}(y)}{4\sqrt{2\pi}} \sum_{n=1}^{\infty} n \int_{-\infty}^{\infty} \int_{-\infty}^{\infty} \alpha_n(p) \frac{J_n(qa)}{q} e^{i(qx + h|y| + pz)} dq dp. \tag{26}$$

The integral in equation (24) is zero for  $m + n$  equal to an odd integer whereas for  $m + n$  even,  $Q_{nm}$  can be evaluated according to

$$Q_{nm} = (-1)^m n m \sqrt{\frac{\pi}{2}} [I_1 + iI_2]. \tag{27}$$

$I_1$  is given by [11]

$$\begin{aligned} I_1 &= \int_0^{\sqrt{k^2 - p^2}} \frac{\sqrt{(k^2 - p^2) - q^2}}{q^2} J_n(qa) J_m(qa) dq \\ &= \frac{1}{2} (a\sqrt{k^2 - p^2})^{m+n} \Gamma(3/2) \Gamma([n + m - 1]/2) / \Gamma([m + n + 2]/2) \Gamma(1 + m) \Gamma(1 + n) \\ &\quad \times {}_3F_4([n + m - 1]/2, [n + m + 1]/2, (n + m)/2 + 1; m + 1, n + m + 1, \\ &\quad \times n + 1; -a^2(k^2 - p^2)), \end{aligned} \tag{28}$$

where  $\Gamma$  is the Gamma function and  ${}_iF_j(\alpha_1, \dots, \alpha_i; \beta_1, \dots, \beta_j, z)$  is the generalized hypergeometric function of order  $(i, j)$  and argument  $z$ .  $I_2$  is given by [12]:

$$\begin{aligned} I_2 &= \int_{\sqrt{k^2 - p^2}}^{\infty} \frac{\sqrt{q^2 - (k^2 - p^2)}}{q^2} J_n(qa) J_m(qa) dq = - \int_0^{\sqrt{k^2 - p^2}} \frac{\sqrt{(k^2 - p^2) - q^2}}{q^2} \\ &\quad \times \left[ J_{>}(qa) Y_{<}(qa) + \frac{\delta_{nm}}{n\pi} \right] dq - \frac{\delta_{nm}}{2n}, \end{aligned} \tag{29}$$

where  $<, > = \min, \max(n, m)$ ,  $Y$  the Bessel function of the second kind, and  $\delta$  is the Kronecker symbol.

Taking  $v = 0$  in the relation

$$x dH_v^{(1)}(x)/dx - vH_v^{(1)}(x) = -xH_{v+1}^{(1)}(x) \tag{30}$$

into the expression for  $T_m$  in equation (25) gives

$$T_m = y_s \sqrt{k^2 - p^2} \int_{-a}^a \varphi_m\left(\frac{x}{a}\right) \frac{H_1^{(1)}(\sqrt{(k^2 - p^2)[(x - x_s)^2 + y_s^2])}}{\sqrt{(x - x_s)^2 + y_s^2}} dx, \tag{31}$$

where one finds the Hankel function of the first kind and first order  $H_1^{(1)} = J_1 + iY_1$ . The integration operation in this last equation can be performed numerically without any major difficulties, provided the co-ordinates of the source  $x_s$  and  $y_s$

do not make the argument of the Hankel function equal to zero, to avoid the singularity of  $Y_1(0)$ . This can be achieved by choosing, for instance,  $y_s$  not equal to zero.

The infinite system of equations in equation (23) must of course be truncated at some  $n_{\max}$ ,  $m_{\max}$  and this raises questions about the convergence of the field in equation (26). The convergence has been tested for typical experimental parameters in practical cases and it was found that the dimension of the system of equations was somehow frequency dependent. To achieve a satisfactory stability of the calculated scattered field, the number of equations was estimated to be no less than about  $ka + 5$ .

However, it is a difficult task, if possible at all, to determine an exact, closed form of the scattered field  $u$  due to the fact that the different coefficients  $\alpha_n$  could be calculated for specific values of the parameter  $p$ , which according to equation (4) may take all possible real values. Thus, one finds again all these values of  $p$  to be taken once more into account in the expression for  $h$  in equation (10) in order to be able to calculate the integral in equation (26). So, to solve this problem as efficiently as possible, one should normally assign the values of the  $\alpha_n$ s by solving the system in equation (23) for all the required values of  $p$  and then insert in equation (26) these  $\alpha_n$  values corresponding to each value of  $p$  for which they were determined. Here, the integration is to be performed relative to the variable  $q$ , whereafter the second integration is to be replaced by some process of convergence acceleration of the summation over the limited number of the  $q$ -integrations resulting from the limited number of the  $p$  values.

On the other hand, and for practical considerations, it is a good first approximation to consider the far field case, namely the case where the field point is so far from the strip that the phase of the integrand in equation (26) oscillates rapidly. In this case the double integration may be performed approximately by means of the two-dimensional stationary phase method. This technique states that if in the integral

$$I = \iint_{-\infty}^{+\infty} A(x, y) e^{i\psi(x, y)} dx dy \quad (32)$$

$\psi \rightarrow \infty$ , then [13]

$$I \cong (2\pi A(x_0, y_0) / \sqrt{|J_0|}) e^{i(\psi(x_0, y_0) + \epsilon\pi/2)}, \quad (33)$$

where  $x_0$  and  $y_0$  are the co-ordinates of the stationary point of the phase and,  $\epsilon = -1, 0, +1$  depending on whether the stationary point is a maximum, saddle point or a minimum.  $J_0$  is the Jacobian at the stationary point (not to be confused with the Bessel function) and is defined by:

$$J_0 = (\partial^2\psi/\partial x^2) \partial^2\psi/\partial y^2 - (\partial^2\psi/\partial x \partial y)^2, \quad (x, y) = (x_0, y_0). \quad (34)$$

If one uses spherical co-ordinates for  $x$ ,  $y$  and  $z$ ,

$$x = r \sin \theta \cos \phi, \quad y = r \sin \theta \sin \phi, \quad z = r \cos \theta, \quad (35)$$

then the phase of the exponential term in equation (26) may be expressed as

$$\psi = r(q \sin \theta \cos \phi + |\sin \theta \sin \phi| \sqrt{k^2 - q^2 - p^2} + p \cos \theta). \tag{36}$$

The co-ordinates of the stationary phase point are the values  $p_0$  and  $q_0$  for  $p$  and  $q$  making the respective derivatives of the phase  $\psi$  change sign: i.e.,

$$\partial\psi/\partial q = 0 \Rightarrow \sin \theta \cos \phi - q|\sin \theta \sin \phi|/\sqrt{k^2 - q^2 - p^2} = 0, \tag{37.1}$$

$$\partial\psi/\partial p = 0 \Rightarrow \cos \theta - p|\sin \theta \sin \phi|/\sqrt{k^2 - q^2 - p^2} = 0. \tag{37.2}$$

If one considers the case where  $y \leq 0$ , equations (37) lead to

$$p_0 = k \cos \theta, \quad q_0 = k \sin \theta \cos \phi, \tag{38}$$

which when inserted in equation (34) permits one to evaluate the Jacobian as

$$J_0 = 1/(rk \sin \theta \sin \phi)^2. \tag{39}$$

The nature of the stationary point is determined from checking at the same time the sign of both the Jacobian and that of the phase's second derivative ( $\partial^2\psi/\partial q^2$ ) at this point. In the present case the stationary point is a maximum and the value of  $\epsilon$  in equation (33) is therefore  $\epsilon = -1$ . The same results are found to apply as well for  $y \geq 0$ .

The coefficients  $T_m$  in equation (25) constituting the right hand side of the system of equations (23) can also be calculated approximately for large arguments of the Hankel function in equation (31). In fact, upon noting that [14]

$$H_1^{(1)}(x) \underset{x \rightarrow \infty}{\cong} \sqrt{(2/\pi x)} e^{i(x - 3\pi/4)}, \tag{40}$$

$T_m$  becomes approximately given by

$$T_m \cong -(1 + i)y_s \left( \frac{k^2 - p^2}{\pi^2} \right)^{1/4} \int_{-a}^a \varphi_m \left( \frac{x}{a} \right) \frac{e^{i\sqrt{(k^2 - p^2)[r_s^2 - 2xx_s + x^2]}}}{(r_s^2 + x^2 - 2xx_s)^{3/4}} dx, \tag{41}$$

where  $r_s^2 = x_s^2 + y_s^2$ . If one further assumes in the integrand that  $r_s^2 \gg x^2$ ,  $2xx_s$  in both the argument of the exponential and in the denominator, a condition which could be satisfied for instance for a point source facing the mid-line of the strip, far away from it, then

$$T_m \cong -(1 + i)y_s \left( \frac{k^2 - p^2}{\pi^2 r_s^6} \right)^{1/4} \int_{-a}^a \varphi_m \left( \frac{x}{a} \right) e^{i\sqrt{k^2 - p^2} r_s (1 - xx_s/r_s^2)} dx, \tag{42}$$

which through using equation (18) gives

$$T_m \cong -(1 + i)(my_s/x_s) \sqrt{\pi/r_s} \sqrt{k^2 - p^2} J_m(\sqrt{k^2 - p^2}[x_s a/r_s]) e^{ir_s \sqrt{k^2 - p^2}}. \tag{43}$$

In this case the term  $e^{ir_s \sqrt{k^2 - p^2}}$  in the coefficients  $T_m$  will have an effect on the values of the  $\alpha_n$ s, and thereupon on the value of the scattered field in equation (26). Still, the two-dimensional stationary phase method can be applied to

the double integration, but here one has the phase of the exponential function  $\psi$  given by

$$\psi = qx + \sqrt{k^2 - q^2 - p^2}|y| + pz + r_s \sqrt{k^2 - p^2}. \quad (44)$$

Here, the determination of the co-ordinates of the stationary phase point may be a little more tedious than in the previous case and the numerical solution for  $p_0$  and  $q_0$  making  $\partial\psi/\partial p = \partial\psi/\partial q = 0$  is sometimes justified, whereafter these values are used in the expression of the Jacobian to determine the nature of the stationary point. In the present case, the calculations are relatively easy and the new co-ordinates of the stationary point for the phase are

$$p_0 = \frac{kz}{\sqrt{r_s^2 + r^2 + 2r_s \sqrt{x^2 + y^2}}}, \quad q_0 = \frac{kx}{\sqrt{x^2 + y^2}} \frac{r_s + \sqrt{x^2 + y^2}}{\sqrt{r_s^2 + r^2 + 2r_s \sqrt{x^2 + y^2}}}. \quad (45)$$

## 5. APPROXIMATE SOLUTION USING THE BIOT-TOLSTOY THEORY OF DIFFRACTION

Most of the solutions to the problems of scattering by a strip have been given for the two-dimensional case. Examples of such approaches are by use of the Wiener-Hopf technique or by means of field expansions in the Mathieu functions [15]. Another approach to such problems has also been recently presented for the case of a normally incident plane wave on the hard strip [16]. This solution is a special application, applied originally to the case of the truncated wedge and consists of combining the exact solution to the problem of diffraction by a vertex with an algorithm for taking into account the multiple diffraction between the two vertices.

In this section, another approach is used which basically is intended for the cases dealing with semi-infinite wedges, but at the same time treats the more general case of spherical wave incidence. This theory gives solutions in the time domain and these are valid for all frequencies [17]. The shortcomings in implementing this method to the strip arise as in the aforementioned case of the truncated wedge, essentially from considering the two edges of the strip as those of semi-infinite half planes. However, taking into consideration the multiple diffraction between the edges partly remedies this problem. Moreover, the order of the multiple diffraction is hard to extend above double diffraction. In reference [16], the results of some calculations on the scattering by a hard strip have been presented. There, the field point was considered to be in the shadow zone of the strip and comparisons were made to the results presented in reference [18]. Thus consider only this latter approach is considered here.

Biot and Tolstoy more than four decades ago presented a new solution to the problem of spherical wave diffraction by a hard wedge [17]. The attractiveness of this theory, subsequently referred to as the B-T theory, is that its formulation is in the time domain and that it uses relatively simple mathematics for the expression of the diffracted field. Consider, as in Figure 2, an infinite hard wedge with angle  $\theta_w$  in a fluid with density  $\rho$  and where the sound speed is  $c$ .

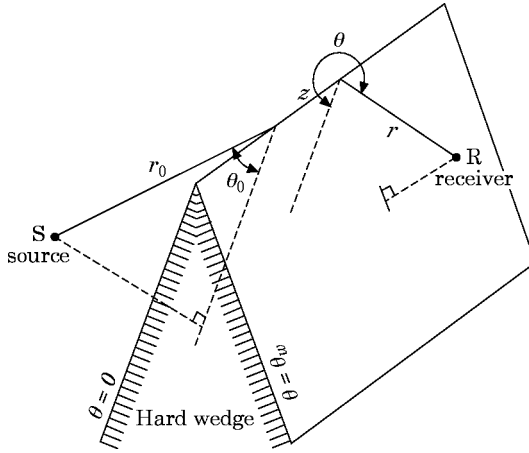


Figure 2. Geometry for the diffraction of a spherical wave by a hard wedge.

If at the point S is emitted an instantaneous pulse of pressure  $p_\delta$ ,

$$p_\delta = (\rho S/4\pi R) \delta(t - R/c), \tag{46}$$

where  $S$  is the strength of the source and  $R$  the distance range to the receiver, then, at a later time  $\tau_0$ , (being the least travel time from the source to the receiver via the crest of the wedge) given by

$$\tau_0 = [(r + r_0)^2 + z^2]^{1/2}/c, \tag{47}$$

the receiver R would detect a disturbance  $p_d(t)$  originating from the tip of the wedge,

$$p_d(t) = (-S\rho c/4\pi\theta_w)\{\beta\}(rr_0 \sinh(Y))^{-1} \exp(-\pi Y/\theta_w), \tag{48}$$

in which  $\beta$  is the sum of terms

$$\beta = \sin[(\pi/\theta_w)(\pi \pm \theta \pm \theta_0)]\{1 - 2 \exp(-\pi Y/\theta_w) \cos[(\pi/\theta_w)(\pi \pm \theta \pm \theta_0)] + \exp(-2\pi Y/\theta_w)\}^{-1}, \tag{49}$$

and

$$Y = \text{arccosh}([(c^2 t^2 - (r^2 + r_0^2 + z^2)]/2rr_0). \tag{50}$$

For the half plane,  $\theta_w = 2\pi$  and equation (48) becomes, for the important case of the half plane with  $z = 0$  [19, 20],

$$p_d(t) = \frac{-S\rho}{4\pi^2 c} \sqrt{\frac{t_+^2 - t_-^2}{t^2 - t_+^2}} \left\{ \frac{\cos \pm}{t^2 - t_+^2 + (t_+^2 - t_-^2) \cos \pm} \right\}_+, \tag{51}$$

where  $t_\pm = (r \pm r_0)/c$  and  $\cos \pm = \cos[(\theta \pm \theta_0)/2]$ . For notational convenience, the term  $\{ \}_+$  in equation (51) is the sum of two terms corresponding to the different signs in the argument of the trigonometric function. It may also be noted that in the case where the source and the receiver lie in the same plane normal to the edge of the half plane one has  $t_+ = \tau_0$ . To date, the exact Fourier transform of the time

domain expression in equation (48) is not available and so one must resort to numerical techniques.

An application of the solution of the wedge problem to the strip of Figure 1 would require generating the strip from a truncated wedge of top width  $2a$  and then letting its angles go to  $2\pi$ . This primary solution may be improved by considering the interaction between the edges of the strip through adding a double diffraction algorithm to the single diffraction solution. When the source illuminates one edge, it in a way stimulates an infinite number of secondary sources, SS's, on the diffracting edge, which in their turn emit their wavelets to the receiver. The strength of these wavelets decays rapidly as one moves on the edge away from the point at the shortest source-edge-receiver distance. This interpretation is supported by the fact that the pressure field as expressed by equation (48) is null for  $t < \tau_0$  and then has an infinitely long wake starting from infinity at  $t = \tau_0$ , diminishing rapidly in amplitude at increasing times.

As a coarse first approximation, the diffracted pressure may then be discretized as if it were resulting from the infinite number of secondary sources on the first edge, emitting at successive discrete time intervals. The double diffracted field is then the build-up of the pressures resulting from the diffraction of these first order waves on the second edge [18]. The secondary sources (SS)  $S_0, S_1, S_n \dots$  are situated on the first edge in such a way that the successive distances source-receiver via the SS's, and then the second edge, lag one another by  $\Delta T$ , the distance  $S_n$ -second edge-receiver being of course the shortest. Then, the mean pressure due to each SS is calculated according to

$$\langle p(n\Delta T) \rangle = \frac{1}{\Delta T} \int_{(n-1/2)\Delta T}^{(n+1/2)\Delta T} p(t) dt, \quad (52)$$

where  $\Delta T$  is the discretizing time corresponding to the Nyquist frequency. This last field is then normalized by

$$p_\delta = \rho S / 4\pi R \Delta T \quad (53)$$

to associate to each SS a strength

$$S_{ssn} = F_n S, \quad F_n = \frac{1}{2} \langle p(n\Delta T) \rangle / p_\delta. \quad (54)$$

There is some controversy about how many SS's to take into consideration in the double diffraction algorithm, but from numerical tests it was found that the few in the immediate neighborhood of the central one are of most significance. As a simple rule it is in general sufficient to take into account only those SS's whose pressure would correspond to  $p_{final} \leq 0.05p(0\Delta T)$ , in accordance with the argument in reference [18]. Moreover, it was noted also from the numerical tests that considering more than the second order diffraction loads the computation without any appreciable improvement of the amplitude of the total field as predicted by the double diffraction.

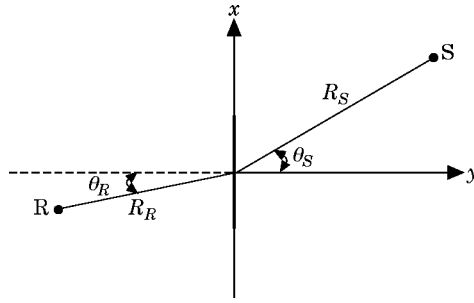


Figure 3. Geometry for the calculation of the scattered field. S is the source and R the receiver. The strip is of width  $2a$ .

6. NUMERICAL EXAMPLES

Some numerical examples are considered in this section for comparing the theoretical predictions made by the exact potential theory to those of the approximate approach using the exact B-T theory of the half plane for the strip. For this latter, a transformation into the frequency domain of the time domain expression in equation (48) is needed. This was done by means of the NAG software package which includes a varied assortment of high precision quadrature subroutines [21].

The scattered field by the strip is defined in this context as the contribution to the total field due to the existence of strip. Hence, if one denotes by  $u_{with}$  and  $u_{without}$  the pressures respectively with and without the strip, the scattered pressure  $u_{scat}$  would then be given by

$$u_{scat} = u_{with} - u_{without} . \tag{55}$$

In order to be able to give a more qualitative and quantitative presentation of the numerical results, the scattered pressure is presented as normalized to the pressure without the strip, i.e., the quantity presented in the figures is the logarithm to the base 10 of

$$|u_{scat} / u_{without}| = |u_{with} / u_{without} - 1| . \tag{56}$$

With respect to the double diffraction, the number of secondary sources is somehow dependent on the frequency of interest because for shorter wavelengths the mutual interference between the waves sent by the secondary sources decreases

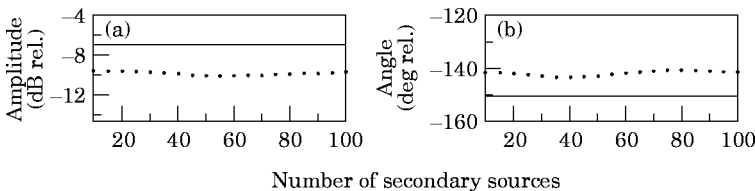


Figure 4. Amplitude and phase of the multiply diffracted field for the case in Figure 3 for  $ka = 1$ . —, Single diffraction; ●●●●, multiple diffraction. Left amplitude, and right phase.

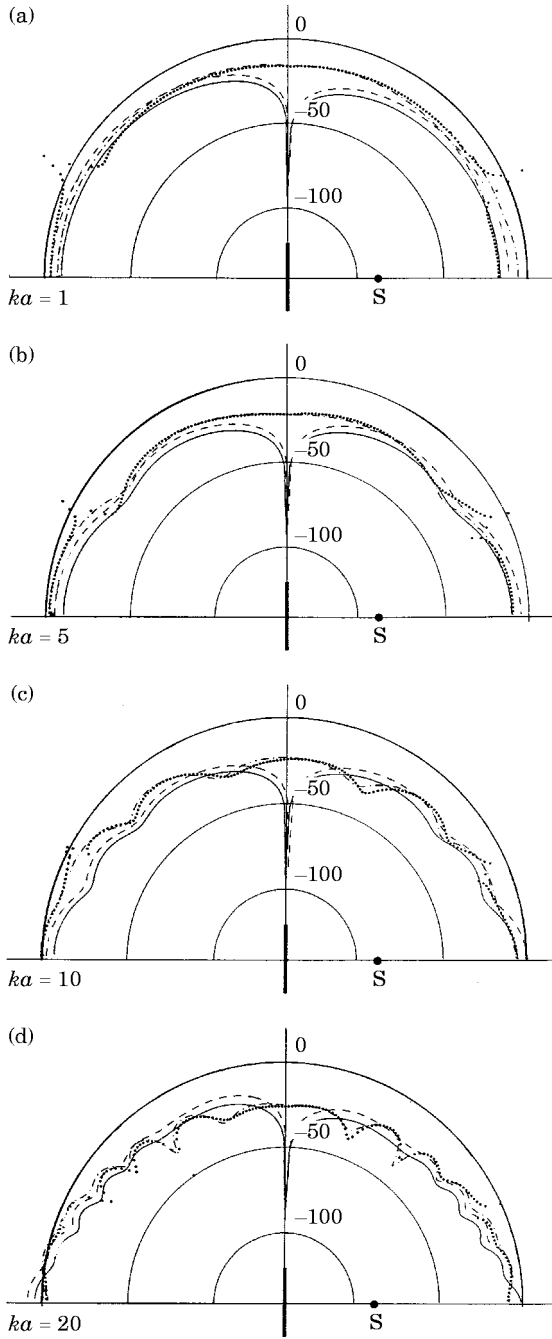


Figure 5. Polar diagrams for the amplitude of the scattered field normalized to the direct field; geometry corresponding to Figure 3; far field: -----, equation (38) and ———, equation (45). B-T theory: ·-·-·-·-·, single diffraction and ●●●●, multiple diffraction.

the significance of their contribution to the total field. Consequently, the corresponding improvement brought to the total diffracted field would be rather limited to the low components of the frequency spectrum.

As a first case of study, calculations of the scattered field were made for the geometry in Figure 3 for different values of the angle  $\theta_R$ .

First, for the B–T approach, a check was made on the stability of the multiple diffracted field at taking an increasing number of SSs. As a result and which is illustrated in Figure 4, already at a frequency such that the strip is about one third wavelength wide, the value of the diffracted field stabilizes at the first few secondary sources. Hence, considering more than around 20 of the strongest SSs would unnecessarily load the computations.

In Figure 5, and as a first application, evaluations were made for the amplitude of the scattered field for a varying polar angle  $\theta_R$  with values ranging from 0 (front scattering, receiver in shadow) to  $\pi$  (back scattering) and for different values of  $ka$ ,  $k$  being the wavenumber and  $a$  half the width of the strip.

For both theoretical approaches, the polar curves fit relatively well, especially at the lower  $ka$  values. At the lateral receiver positions it is difficult to decide on which approach has the better prediction for both of them become somehow unreliable at these positions. Regarding the potential theory approach, this is due to the various approximations made for the calculations especially those which led to equation (41). On the other hand, and for the approximate approach built on the half plane solution, a more in depth examination of the sources of errors may be needed. To elaborate a little more on this and to take as an example the already worked out problem of the plane wave scattering by a thin hard free hanging strip, the scattered field in this case attains its minimum value of zero for tangential wave incidence; the wave impinging on the strip at grazing incidence resumes its way as if it were unaware of the presence of the strip [22]. According to the reciprocity principle, the scattered field would then also be null in the plane of the strip whatever the direction of the incident wave. With reference to Figure 5, this is obviously satisfied for the potential theory solution but not for the approximate solution. For this latter, neither the single nor the multiple diffraction part of the scattered part is null in the plane of the strip. For an observation point situated in this plane, the field diffracted by one edge of the strip is zero in the half plane extending away from this edge and not containing the other edge (this could be proved through setting  $\theta = \pi$  in equation (51)). On the other hand, the diffracted field is not null in the complementary half plane ( $\theta = 0$  in equation (51)).

For the potential theory approach, the far field solution (equation (38)) exhibits a somewhat larger value than in the case where both source and receiver are at distances of the same order from the strip (equation (45)). Both curves lie parallel to each other with a distance depending only on the geometry of the case under study. This is a consequence of the fact that both approximations differ only in the value of the second coordinate of the stationary point (value of  $q$  in equation (26)).

In the results from the B–T theory, the multiple diffraction, although contributing a great deal to the total scattered field at the low frequencies, proves to be of low efficiency at higher  $ka$  values. Another shortcoming of the actual formulation of the multiple diffraction is that it performs poorly in the transition region between the uninsonified to the insonified regions, or at the boundary for these regions corresponding to the image of the source through the strip. These regions should normally have no real physical significance, and the failures in them

are merely the consequence of applying the multiple diffraction treatment. In fact, as the observation point penetrates the geometrical boundary, the slope of the frequency curve of the diffracted energy moves from  $f^{-1/2}$  at large angles to a flat spectrum  $f^0$ , corresponding thus to a delta function in the time domain [18]. This singular behaviour of the diffracted field is inherent in its formulation, equation (48), in order to fulfill the continuity of the total field when moving across the geometrical boundaries. These transition zones are also found to be somewhat dependent on frequency as one notices that their angular size diminishes the higher the frequency. It is thus advised to discard using multiple diffraction at such zones. As in almost all cases of diffraction, one notices also the appearance of scattering lobes in the response curves bringing into evidence the directivity characteristics of the scattered field. The higher the frequency, the greater the number of lobes. This feature is found in practically almost all cases of diffraction by objects having two or more parallel diffracting edges and, in terms of geometrical optics, a direct and plausible explanation may be found in the mutual interference between the waves propagating from the diffracting edges. In the case of Figure 5, the scattering lobes have a more or less periodic pattern for  $ka > \pi/2$  (strip width larger than a half wavelength). For lower values of the frequency, the path difference from source to receiver past the edges is less than  $\lambda/2$  and no interference phenomena can occur; hence no lobe may be observed; Figure 5(a) for  $ka = 1$ . For

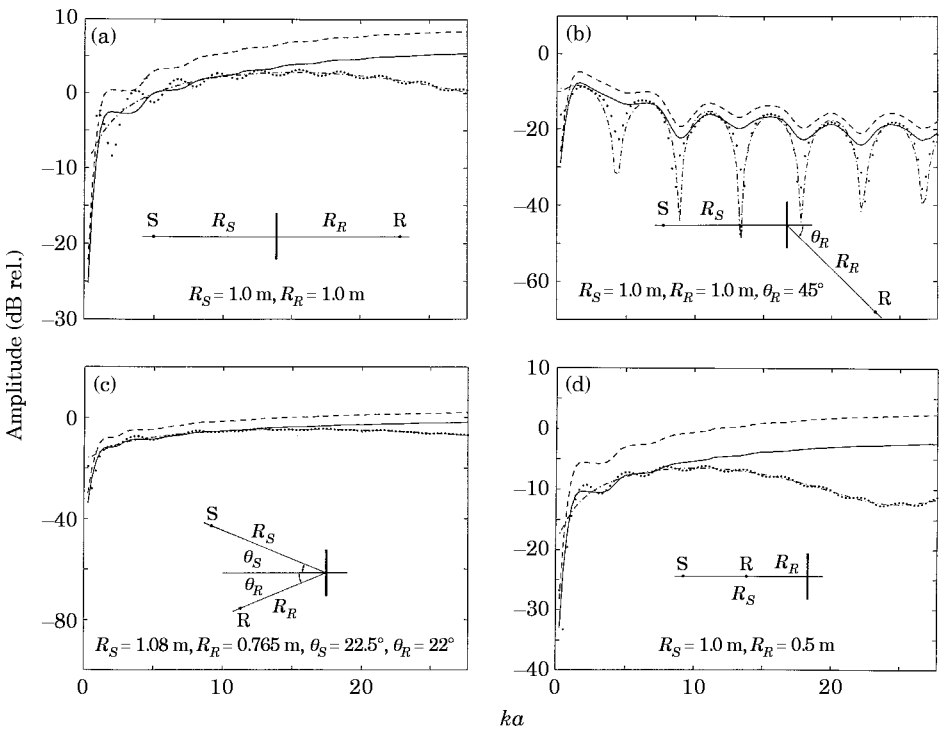


Figure 6. Amplitude of the scattered field *re* free field for different combinations of source and receiver positions. Strip width  $2a = 30 \text{ cm}$ . Potential theory approach: ---, equation (38), and —, equation (45). B-T theory: ·-·-·, single diffraction, and ●●●●, multiple diffraction.

shorter and shorter wavelengths, the lobes become sharper and more pronounced with an angular periodicity  $\Delta\theta$  satisfying approximately  $2a\Delta\theta = \lambda$ , where  $2a$  is the width of the strip and  $\lambda$  the wavelength.

In Figure 6, the results of similar calculations on the scattered field for fixed positions of the source and the receiver are plotted against frequency as a function of  $ka$ . A value of  $ka = 3$  corresponds approximately to a strip width equal to one wavelength.

A first important observation to be made is that the scattering, as opposed to the edge diffraction of sound waves is rather a high frequency phenomenon. In fact, as expressed in equation (56), one can deduce from Figure 6 that for very low frequencies the amplitude of the scattered field takes on negligible values whereas at higher frequencies it tends towards its geometrical optics value. For all the cases considered in this study, scattering starts to exhibit rather abruptly its strongest behaviour for frequencies corresponding to a strip width equal to about half a wavelength. As the frequency is increased, the amplitude of the scattered field for the forward and back scattering becomes smaller after a maximum at a  $ka$  value of around 10–15. This is well seen in the case of forward scattering, Figure 6(a), where for very short wavelengths the value of the scattered field tends, with an opposite phase, to that of the incident field and the curve of the amplitude approaches the value 0. This trend is less well marked in the case of backward scattering; see Figure 6(d), where the wave is incident in a direction normally to the strip. In this case, both the backscattering and the specular directions coincide and the scattered pressure is at the maximum of its amplitude, i.e., the value of the scattered field tends to that of the specularly reflected field, and in both these latter cases the edge diffracted phenomenon becomes less and less significant for higher frequencies.

The solution of the integral equation, equation (15), gives satisfactory results for values of  $ka$  up to about 15 (strip about 5 wavelengths wide). Again, the predictions for the scattered field resulting from equations (38) and (45) follow each other in a perfectly parallel manner and are only some dBs apart due to the different values of the co-ordinate  $q$  of the stationary point in equation (26).

There is also to be noticed a quite strong interference pattern in the forward scattering when both edges of the strip lie in proximity to the sight line joining the source to the receiver. In this geometrical configuration of the experiment, see Figure 6(b), the scattered field in the geometrical optics sense is the sum of the contributions from the edge waves generated at the sharp straight parallel boundaries of the strip. These two components have about the same amplitudes; hence the comb filter effect resulting from their superposition. This is in a way as similar to Young's earlier experiment on the interference of light by two parallel narrow slits in an opaque screen. In this famous optical experiment, the interference pattern occurs in space whereas in our case one can easily calculate the frequency in the periodicity of the interference pattern as being approximately equal to  $ka \approx \pi/\cos(\theta_R) = \sqrt{2}\pi$ . This phenomenon, also commonly known as Fresnel diffraction is due to the relatively large amplitude of the edge diffracted wave at the geometrical boundaries of the incident field, the magnitude of which may be of the same order as that of the incident field. The envelope of the

scattering curve is also seen in this case to decrease in amplitude for shorter wavelengths, which confirms again the lesser significance of the edge diffraction phenomenon for increasing frequencies. The interference between the edge diffracted waves, although also present near the geometrical boundary of the reflected wave, does not manifest itself in the case of Figure 6(c) simply because it is almost completely masked by the stronger wave which is specularly reflected by the strip. In this latter case, a plane hard scatterer may be considered as an ideal reflector when, according to a Huygens' construction of the Fresnel zones, it contains at least half of the innermost Fresnel zone [23], a condition which is satisfied for the present strip at  $ka \approx 11$ . The interference of the edge waves has a negligible contribution to the scattered field in the case of Figure 6(a) because the receiver, being situated on the normal passing through the middle of the strip, is at equal distances from both its edges and the diffracted pressures emanating from them are consequently in phase for all frequencies. The same reasoning applies as well for the case of backscattering in Figure 6(d).

## 7. CONCLUSIONS

In this paper the problem of scattering of a spherical wave by a thin hard strip has been solved by means of an integral equation method. The unknown in the integral equation is the potential jump across the strip which is expanded in some appropriate functions, with account taken of the surface potential behaviour at the edges of the strip. The formulation is direct and the numerical implementation, which for the far field case is relatively easy, permits the treatment of quite high frequencies. An approximate approach in which an exact solution of the diffraction problem by a half plane is used, has also been presented and compared to the actual solution. It is shown that such approximate solutions, even when taking account of the multiple diffraction between the edges of the strip, may give substantial errors in estimating the scattered field at observation points approaching the plane of the strip. Using the potential theory gives the right prediction for such cases.

## ACKNOWLEDGMENT

The author is very much indebted to Professor Anders Boström at the Chalmers University of Technology, Gothenburg for valuable hints and for his continuous and kind assistance during the achievement of this work.

## REFERENCES

1. C. J. BOUWKAMP 1954 *Reports on Progress in Physics* **17**, 35–100. Diffraction theory.
2. M. BORN and E. WOLF 1986 *Principles of Optics* (Sixth edition). Headington, Oxford: Pergamon Press.
3. F. CASSOT and G. P. EXREMET 1972 *Acustica* **27**, 238–245. The numerical determination of the sound field and of the characteristic frequencies in a circular enclosure by the method of discretisation.

4. P. J. T. FILIPPI 1977 *Journal of Sound and Vibration* **54**, 473–500. Layer potentials and acoustic diffraction.
5. P. FILIPPI and G. DUMERY 1969 *Acustica* **21**, 343–350. Etude theorique et numerique de la diffraction par un écran mince.
6. F. CASSOT 1975 *Acustica* **34**, 64–71. Contribution a l'étude de la diffraction par un écran mince.
7. A. DAUMAS 1978 *Acustica* **40**, 213–222. Etude de la diffraction par un écran mince disposé sur le sol.
8. A. BOSTRÖM 1991 *Journal of the Acoustical Society of America* **90**, 3344–3347. Acoustic scattering by a sound-hard rectangle.
9. A. BOSTRÖM and L. PETERSON 1991 *Journal of the Acoustical Society of America* **90**, 3338–3343. Scattering of acoustic waves by a circular disc in the interface between two fluids.
10. H. HÖNL, A. W. MAUE and K. WESTPHAL 1961 *Handbuch der Physik* **25**. *Theori der Beugung*, Berlin: Springer Verlag.
11. A. P. PRUDNIKOV, Y. A. BRYCHKOV and O. I. MARICHEV 1986 *Integrals and Series* **II**, New York: Gordon and Breach Science Publishers; see p. 212, formula 2.12.32-3.
12. P. M. VAN DEN BERG 1986 *Journal of the Acoustical Society of America* **70**, 615–619, Transition matrix in acoustic scattering by a strip.
13. H. BREMMER 1949 *Terrestrial Radio Waves*. New York: Elsevier.
14. M. ABRAMOVITZ and I. STEGUN 1972 *Handbook of Mathematical Functions*. New York: Dover Publications, see p. 364, formula 9.2-3.
15. J. J. BOWMAN, T. B. A. SENIOR and P. L. E. USLENGHI 1987 *Electromagnetic and Acoustic Scattering by Simple Shapes*. New York: Hemisphere Publishing Corporation, see chapter *The Strip*.
16. I. TOLSTOY 1989 *I.E.E.E. Journal of Oceanographic Engineering* **14**, 4–16. Diffraction by a hard truncated wedge and a strip.
17. M. A. BIOT and I. TOLSTOY 1957 *Journal of the Acoustical Society of America* **29**, 381–391. Formulation of wave propagation in infinite media by normal coordinates with an application to diffraction.
18. H. MEDWIN, E. CHILDS and G. M. JEBSEN 1982 *Journal of the Acoustical Society of America* **72**, 1005–1013. Impulse studies of double diffraction: a discrete Huygens interpretation.
19. H. MEDWIN 1981 *Journal of the Acoustical Society of America* **69**, 1060–1065. Shadowing by a finite barrier.
20. D. OUIS 1997 Report TVBA 3094, *Department of Engineering Acoustics, Lund Institute of Technology, Sweden*. Theory and experiment on the diffraction by a hard half plane.
21. THE NUMERICAL ALGORITHM GROUP 1985 *NAG Mark 15*. Oxford.
22. P. MORSE and H. FESCHBACH 1953 *Methods of Theoretical Physics*. **II**, Tokyo: McGraw-Hill; see pp. 1428–1432.
23. L. CREMER and H. MÜLLER 1982 *Principles and Applications of Room Acoustics* **1**. London: Applied Science Publishers.
24. I. S. GRADSHTEYN and I. M. RYZHIK 1980 *Tables of Integrals, Series and Products*. New York: Academic Press. see p. 472, formulas 3.876-1.2.
25. Reference [24], but see p. 836, formula 7.355-2.

APPENDIX: “FINITE” FOURIER TRANSFORM OF THE RELATED  
CHEBYCHEV “POLYNOMIALS”, EQUATION (18)

The related Chebychev polynomials

$$\varphi_n(x) = \begin{cases} \cos(n \arcsin x) & n = 1, 3, 5, \dots \\ i \sin(n \arcsin x) & n = 2, 4, 6, \dots \end{cases} \quad (\text{A1})$$

are related to the true Chebychev polynomials of the first kind  $T_n(x)$  by

$$T_n(x) = \cos(n \arccos x) \tag{A2}$$

and of the second kind  $U_n(n)U_n(x)$  by

$$U_n(x) = \frac{1}{\sqrt{1-x^2}} \sin((n+1) \arccos x) \tag{A3}$$

through the following. First, with the help of

$$\arccos x + \arcsin x = \pi/2,$$

one can write

$$\varphi_n(x) = \begin{cases} \cos(n\pi/2 - n \arccos x) = (-1)^{(n-1)/2} \sqrt{1-x^2} U_{n-1}(x) & n = 1, 3, 5, \dots \\ i \sin(n\pi/2 - n \arccos x) = i(-1)^{n/2} \sqrt{1-x^2} U_{n-1}(x) & n = 2, 4, 6, \dots \end{cases} \tag{A4}$$

Then,  $U_n$  is related to  $T_n$  through

$$U_n(x) = [1/2(1-x^2)][T_n(x) - T_{n+2}(x)]. \tag{A5}$$

Interest here is in evaluating the integral

$$I = \int_{-a}^a \varphi_n\left(\frac{x}{a}\right) e^{-iqx} dx. \tag{A6}$$

With the change of variable

$$y = (x/a) \Rightarrow dx = a dy \quad \text{and} \quad -a \leq x \leq +a \Rightarrow -1 \leq y \leq +1, \tag{A7}$$

then

$$I = a \int_{-1}^1 \varphi_n(y) e^{-iqay} dy, \tag{A8}$$

and, for  $n$  odd,

$$I = a \int_{-1}^1 (-1)^{(n-1)/2} \sqrt{1-y^2} \frac{1}{2(1-y^2)} [T_{n-1}(y) - T_{n+1}(y)] \times (\cos(qay) - i \sin(qay)) dy. \tag{A9}$$

Moreover, for  $n$  odd,  $T_{n\pm 1}$  is even and  $T_{n\pm 1} \sin$  is odd which gives a null contribution to  $I$ . Thus one is left with

$$I = a(-1)^{(n-1)/2} \int_0^1 \frac{T_{n-1}(y) - T_{n+1}(y)}{\sqrt{1-y^2}} \cos(qay) dy, \tag{A10}$$

which gives [24]

$$I = \frac{\pi a}{2} (-1)^{\frac{n-1}{2}} \left[ (-1)^{\frac{n-1}{2}} J_{n-1}(qa) - (-1)^{\frac{n+1}{2}} J_{n+1}(qa) \right], \tag{A11}$$

and, upon using

$$J_{n-1}(qa) + J_{n+1}(qa) = (2n/qa)J_n(qa), \tag{A12}$$

one gets the final result

$$I = (n\pi/q)J_n(qa). \tag{A13}$$

For  $n$  even,  $T_{n\pm 1}$  is odd and  $T_{n\pm 1} \cos$  is odd which gives a null contribution to  $I$ ; thus

$$I = -a(-1)^{n/2} \int_0^1 \frac{T_{n-1}(y) - T_{n+1}(y)}{\sqrt{1-y^2}} \sin(qay) dy, \tag{A14}$$

which gives [25]

$$I = (\pi a/2)(-1)^{n/2} [(-1)^{n/2-1} J_{n-1}(qa) - (-1)^{n/2} J_{n+1}(qa)], \tag{A15}$$

which in turn, by use of equation (A12), gives equation (A13).

Furthermore one can express, for later use, the integral

$$I' = \int_{-a}^a \varphi_n \left( \frac{x}{a} \right) e^{iqx} dx. \tag{A16}$$

For  $n$  odd,  $\varphi_n = \varphi_n^*$  and

$$I' = \int_{-a}^a \varphi_n^* \left( \frac{x}{a} \right) (e^{-iqx})^* dx, \tag{A17}$$

where  $*$  denotes the complex conjugate. Hence

$$I' = \left[ \int_{-a}^a \varphi_n \left( \frac{x}{a} \right) e^{-iqx} dx \right]^* = \frac{n\pi}{q} J_n(qa). \tag{A18}$$

For  $n$  even  $\varphi_n = -\varphi_n^*$  and

$$I' = -(n\pi/q)J_n(qa). \tag{A19}$$

Equation (A16) can finally be written in a generalized form as

$$\int_{-a}^a \varphi_n \left( \frac{x}{a} \right) e^{iqx} dx = (-1)^{n-1} \frac{n\pi}{q} J_n(qa). \tag{A20}$$